CrossMark

Be STARS IN THE OPEN CLUSTER NGC 6830

Po-Chieh Yu(俞伯傑)[1,2], Chien-Cheng Lin(林建爭)[1,3], Hsing-Wen Lin(林省文)[1], Chien-De Lee(李建德)[1], Nick Konidaris[4], Chow-Choong Ngeow(饒兆聰)[1], Wing-Huen Ip(葉永烜)[1,5], Wen-Ping Chen(陳文屏)[1,6], Hui-Chen Chen(陳慧真)[7], Matthew A. Malkan[2], Chan-Kao Chang(章展誥)[1], Russ Laher(良主嶺亞)[8], Li-Ching Huang(黃立晴)[1], Yu-Chi Cheng(鄭宇棋)[1], Rick Edelson[9], Andreas Ritter[1,10], Robert Quimby[11], Sagi Ben-Ami[12], Eran. O. Ofek[12], Jason Surace[8], and Shrinivas R. Kulkarni[13]

[1] Graduate Institute of Astronomy, National Central University, 300 Jhongda Road, Jhongli 32001, Taiwan
[2] Department of Physics and Astronomy, University of California, Los Angeles, CA 90024, USA
[3] Key Laboratory for Research in Galaxies and Cosmology, Shanghai Astronomical Observatory, Chinese Academy of Sciences, 80 Nandan Road Shanghai 200030, China
[4] Cahill Center for Astronomy and Astrophysics, California Institute of Technology, 1200 E. California Boulevard, Pasadena, CA 91125, USA
[5] Institute of Space Science, National Central University, 300 Jhongda Road, Jhongli 32001, Taiwan
[6] Department of Physics, National Central University, 300 Jhongda Road, Jhongli 32001, Taiwan
[7] Department of Natural Sciences and Sustainable Development, Ministry of Science and Technology, 106, Sec. 2, Heping E. Road, Taipei 10622, Taiwan
[8] Spitzer Science Center, California Institute of Technology, M/S 314-6, Pasadena, CA 91125, USA
[9] Department of Astronomy, University of Maryland, College Park, MD 20742, USA
[10] Department of Astrophysical Sciences, Princeton University, Princeton, NJ 08544, USA
[11] Kavli-Institute for the Physics and Mathematics of the Universe, University of Tokyo, Kashiwanoha 5-1-5, Kashiwa-shi, Chiba, Japan
[12] Department of Particle Physics and Astrophysics, The Weizmann Institute of Science, Rehovot 76100, Israel
[13] Division of Physics, Mathematics and Astronomy, California Institute of Technology, Pasadena, CA 91125, USA

ABSTRACT

We report the discovery of two new Be stars, and re-identify one known Be star in the open cluster NGC 6830. Eleven Hα emitters were discovered using the Hα imaging photometry of the Palomar Transient Factory Survey. Stellar membership of the candidates was verified with photometric and kinematic information using 2MASS data and proper motions. The spectroscopic confirmation was carried out by using the Shane 3 m telescope at the Lick observatory. Based on their spectral types, three Hα emitters were confirmed as Be stars with Hα equivalent widths greater than -10 Å. Two objects were also observed by the new spectrograph spectral energy distribution-machine (SED-machine) on the Palomar 60-inch Telescope. The SED-machine results show strong Hα emission lines, which are consistent with the results of the Lick observations. The high efficiency of the SED-machine can provide rapid observations for Be stars in a comprehensive survey in the future.

Key words: galaxies: star clusters: individual (NGC 6830) – instrumentation: spectrographs – stars: emission-line, Be

1. INTRODUCTION

Be stars are non-supergiant B-type stars with Balmer emission lines, especially the Hα lines. Be stars are also characterized by their fast rotation, color excess at infrared wavelengths, and continuum/emission-line variability (Koubský et al. 1997; Hubert & Floquet 1998; Townsend et al. 2004). Some Be stars show the variability with periods that might be due to pulsation or rotation (Porter & Rivinius 2003; Rivinius et al. 2003). Previous studies have found the enhancement of Be phenomena in young clusters (Wisniewski & Bjorkman 2006; Mathew et al. 2008), while McSwain & Gies (2005) showed an overall increase in Be frequency with age until 100 Myr. McSwain & Gies (2005) also indicated that Be star formation is not strongly related to the cluster density. Furthermore, the Be star fraction in open clusters seems to be increasing with lower metallicity; between 17.5% and 40% of B stars were found to be Be stars in the Large Magellanic Cloud and Small Magellanic Cloud (SMC; see a detailed review in Rivinius et al. 2013).

It is well accepted that the Hα emissions of Be stars originate from the circumstellar material, which is suggested to be a flattened disk (Quirrenbach et al. 1994, 1997; Wood et al. 1997; Carciofi & Bjorkman 2006). The disks are found to be in Keplerian rotation and stable (Kraus et al. 2012; Meilland et al. 2012). The material might be moved from the

stellar surface to form the circumstellar disk (e.g., the decretion disk) through the combination of fast rotation and other mechanisms, such as nonradial pulsations or magnetic fields (Lee et al. 1991; Porter & Rivinius 2003; Townsend et al. 2004; Carciofi et al. 2009). There are several possible origins of the fast rotating star: (1) binary interaction (Pols et al. 1991), by which, during the interaction process, mass and angular momentum can be transferred from the primary star to the mass gainer star, and the latter might be spun-up to a fast rotating star, (2) they might be born as fast rotators, and (3) they have been spun-up during the main-sequence evolution.

To further understand the nature of Be stars, several surveys of Be stars have been carried out in the past (Mclaughlin 1932; Jaschek et al. 1964; Drew et al. 2005; Chojnowski et al. 2015; Lin et al. 2015; Raddi et al. 2015). Because stars in clusters share age and metallicity, Be stars in a sample of clusters with different ages play an essential role in the study of their evolution. Previous studies have searched for emission-line objects in a number of star clusters in the SMC and MW. (Fabregat & Torrejón 2000; Keller et al. 2001; Wisniewski & Bjorkman 2006; Mathew et al. 2008; Martayan et al. 2010; Mathew & Subramaniam 2011). Particularly, McSwain & Gies (2005) provided the most extensive survey of Be stars in the MW; they investigated 55 clusters and concluded that 73% of the rapid rotators might be spun-up by the effect of mass
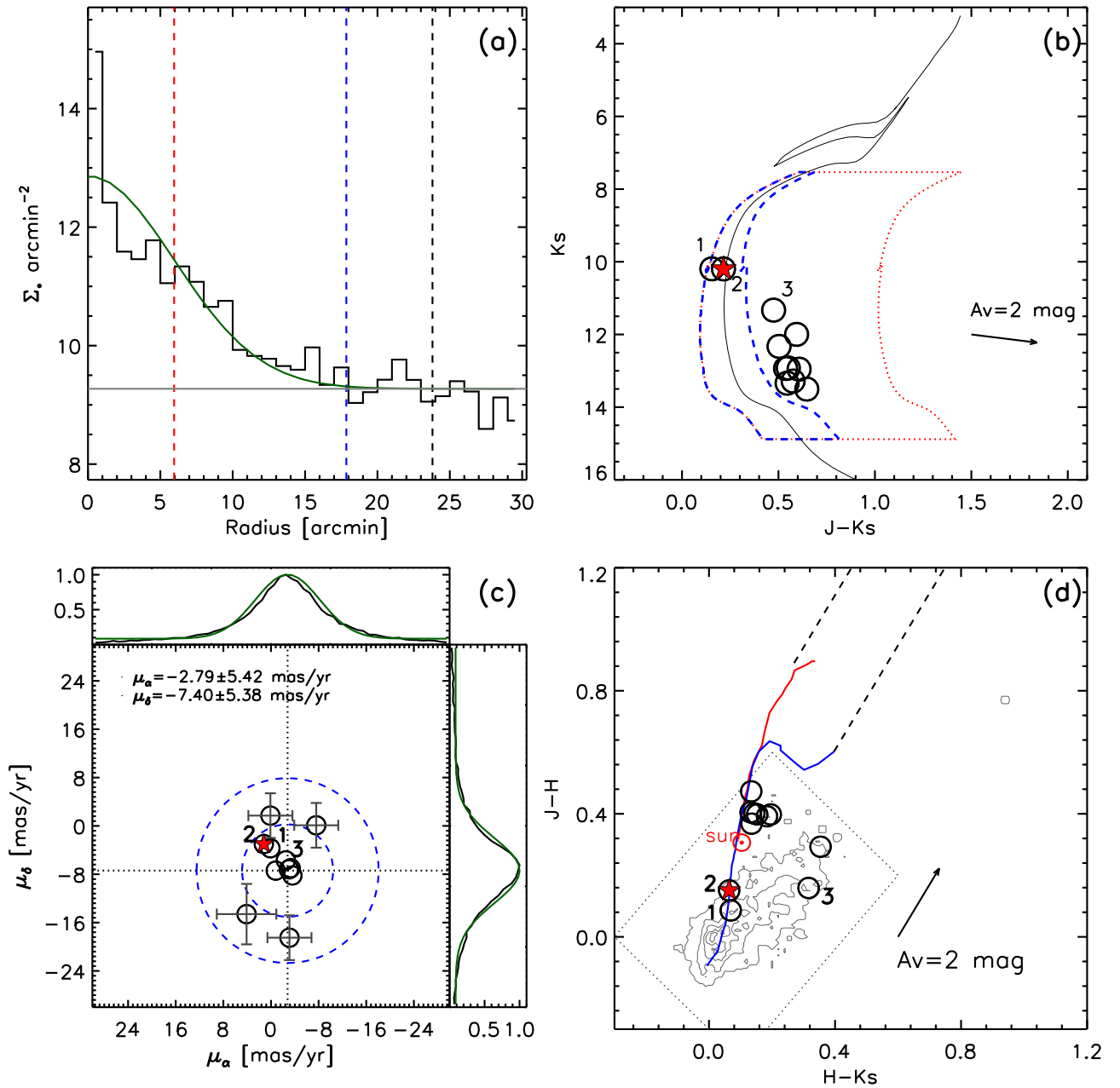
1

Figure 1. Membership identification. In panels (b)–(d), open circles represent our Be star candidates, while the red pentagram is the known Be star VES 72. Numbers represent spectroscopically confirmed Be stars NGC6830-1, NGC6830-2, and NGC6830-3 in this study. (a) Radial density profile of NGC 6830. The gray horizontal line indicates the background density. The green curve shows the best Gaussian fitting results, while red and blue vertical lines represent the widths of 1σ and 3σ. The black vertical line shows the width of the Gaussian curve of 4σ. (b) 2MASS color–magnitude diagram. The black solid line indicates the isochrone (Girardi et al. 2002) of 125 Mys located at 1.8 kpc. Be candidates are considered to have photometric membership within the red-dashed region, while non-emission-line stars are considered to have photometric membership within the blue-dashed region. (c) Stellar PMs distribution of Be candidates of NGC 6830. The PM of NGC 6830 is (μ_α, μ_δ) = (−2.79, −7.40) mas year^{-1}. The inner and outer blue-dashed circles represent $1\sigma_\mu$ and $2\sigma_\mu$ regions. We adopted the 2σ region to define the kinematic membership. The bars are errors of the PMs. The upper and right panels show the μ_α and μ_δ of stars within $48' \times 48'$; green lines show the Gaussian fitting to PMs. (d) 2MASS color–color–magnitude diagram. The gray contours show the known Be stars distribution, and we define the dashed box to select possible Be candidates.

transfer between binaries. Moreover, McSwain et al. (2009) also showed that the distributions of the projected rotational velocity of Be stars and normal B-type stars are significantly different, indicating that they might be different stellar populations, and Be stars cannot be drawn from a sample of normal B stars. Theoretical simulations also imply that most Be stars could be formed during the phase of binary interactions (de Mink et al. 2013; Shao & Li 2014). These studies further supported a spin-up scheme for the evolutionary sequence of Be stars.

Nevertheless, the sample of Be stars in open clusters is far from complete due to a couple of difficulties: (1) a comprehensive spectroscopic survey is time consuming and (2) spectroscopic surveys are often limited to bright stars. Therefore, with the wide field of view (7.3 square degree) of the 48-inch Samuel Oschin Telescope, the Palomar Transient Factory (PTF; Law et al. 2009) project provides an efficient way to search for emission-line candidates in open clusters using Hα imaging photometry (Yu et al. 2015). Furthermore, a new instrument called the spectral energy distribution-machine

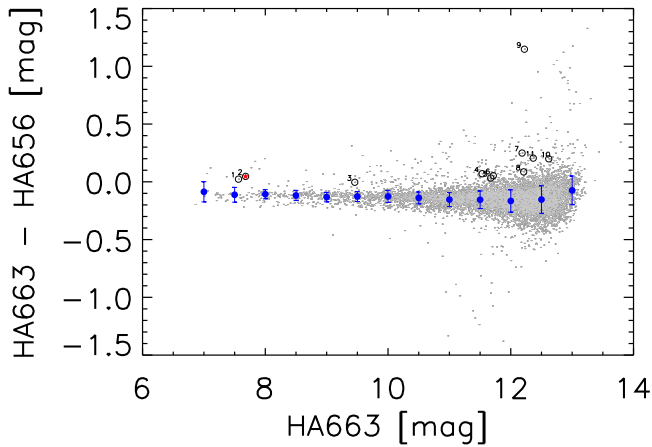**Figure 2.** Hα emitter candidates selection. Gray dots: stars used for calculating photometric scattering; open circles: emission-line candidates with membership confirmation; numbers represent Be candidates NGC6830-1–NGC6830-11; red pentagram: known Be stars VES 72. Blue filled circles represent the mean values of HA663−HA656 within each 0.5 mag bin. The error bars represent the photometric scattering σ_p, which are calculated with the error propagated from photometric and systematic errors. Stars with HA663−HA656 > mean $+2\sigma_p$ are selected as emission-line candidates.

(SED-machine; Ben-Ami et al. 2012; Ngeow et al. 2013; Ritter et al. 2014) provides a possible solution for the fast and efficient follow-up spectroscopic observations for the emission-line candidates found in PTF, because the highly efficient SED-machine is designed to classify transient events rapidly with a low-resolution ($\lambda/\delta\lambda \sim 100$) integrated field unit (IFU) spectrograph that covers a large wavelength range (370–920 nm). Thus, a comprehensive survey of Be stars in star clusters can be accomplished with a combination of the PTF Hα imaging photometry and the SED-machine.

Here we present the results of searching for Be stars in an open cluster NGC 6830 ($\alpha_{2000} = 19^{h}50^{m}59^{s}$, $\delta_{2000} = 23°06'00''$). NGC 6830, located at a distance of 1.8 kpc (Kharchenko et al. 2013) in the constellation Vulpecula (Barkhatova 1957), has a fairly loose structure. In contrast to our previous work (NGC 663 with an age of ~31 Myr, Yu et al. 2015), the age of NGC 6830 is about 125 Myr (Kharchenko et al. 2013) and only one Be star has been reported in this cluster (Hoag & Applequist 1965) prior to our work. Using the relation of effective temperature and age, Peña et al. (2011) determined that the age of NGC 6830 is log(age) = 7.69 years (48.9 Myr) with the hottest star (17,000 K) in the membership of 19 stars. It seems that the age given by Kharchenko et al. (2013) is not consistent with that of Peña et al. (2011). However, while the membership in Peña et al. (2011) is only determined from the distance, Kharchenko et al. (2013) included the proper motions (PMs) to determine the membership and give the log (age) = 8.105 ± 0.062 years (125 Myr). Furthermore, the range of the effective temperature for the membership in Peña et al. (2011) is from 12,000 to 17,000 K, indicating that the log(age) is between 7.69 and 8.22 years, which is also consistent with the age given by Kharchenko et al. (2013). Thus, here we adopted the age given by Kharchenko et al. (2013).

In addition to the age difference, we selected NGC 6830 as the subject of this work because the known Be star is fairly bright and hence it is suitable to be observed with the SED-machine during its commissioning runs. Therefore, the main goal of this work is to demonstrate the capability of the combined PTF Hα imaging photometry, the archival 2MASS

and proper motions data, and the SED-machine in the search of Be stars in open clusters. This will lay the foundation of our future work in this area. In Section 2, we describe the methodology of identifying emission-line stars and the determination of cluster membership using the PTF Hα imaging photometry. In Sections 3 and 4, we describe our spectroscopic observations and present our results based on these observations. Section 5 gives a summary and discussion of this study.

2. IDENTIFICATION OF Be CANDIDATES AND MEMBERSHIP

The methodology of searching for Be star candidates and identifying membership has been presented in our pilot project. Further details can be found in Yu et al. (2015) and will not be repeated here. Briefly, procedures that we followed in this study are summarized below.

1. Determining the searching region based on the radial density profile. The stars were selected from the PPMXL data set with a signal-to-noise ratio (S/N) $\geqslant$ 10 in 2MASS J, H, and K_s bands. The half-Gaussian fitting gives a 3σ radius of $17'.85$ (Figure 1(a)). Because open clusters have irregular shapes, we therefore adopted a box with the side of $48'$ (4σ) as our searching region for NGC 6830 to cover possible candidates.

2. Applying the Hα imaging photometry to identify possible Hα emitters. The Hα emitters should have a more significant flux excess in the on-line image than in the off-line image, where the on-line and off-line images were taken through the HA 656 and HA 663 narrow-band filters. These images were processed for bias corrections, flat-fielding, and astrometric calibration with pipelines developed at the Infrared Processing and Analysis Center (IPAC; Laher et al. 2014). Following the methods and criteria as given in Yu et al. (2015), we selected the Hα emitter candidates that stand out in the plot of the differential HA663−HA656 flux as possible Hα emitters (see Figure 2).

3. Verifying the photometric membership using near-infrared data. The near-infrared J-, H-, and K_s-band data are obtained from the 2MASS point source catalog (Cutri et al. 2003). Possible photometric members of NGC 6830 are determined by selecting stars within the region that are near the isochrone in the 2MASS K_s versus $J - K_s$ color–magnitude diagram (Figure 1(b)). Considering that Be stars might exhibit a large infrared excess (Lee & Chen 2011), we extended the selection region to $J - K_s$ ~1.2 mag (Figure 1(b)) for the Hα emitter candidates.

4. Verifying the kinematic membership using the PMs. Because about 10% of objects in PPMXL data include spurious entries (Röser et al. 2010), Kharchenko et al. (2012) have averaged their PMs and computed errors. Thus, we used PMs provided by Kharchenko et al. (2012) to calculate the averaged PM (μ_α, μ_δ) and standard deviations ($\sigma_{\mu\alpha}$, $\sigma_{\mu\delta}$) of stars within the $47'.6 \times 47'.6$ region by fitting a Gaussian distribution to the PMs. The adopted σ_μ included the error propagated from $\sigma_{\mu\alpha}$ and $\sigma_{\mu\delta}$. Stars were then considered as the kinematic membership if their PMs are within the $2\sigma_\mu$ region (Figure 1(c)).

4

Table 1
Be Candidates

ID	R.A. (hh:mm:ss)	Decl. (hh:mm:ss)	μ_α (mas yr^{-1})	μ_δ (mas yr^{-1})	epm (mas yr^{-1})	K_s (mag)	$J - H$ (mag)	$H - K_s$ (mag)	HA663 (mag)	HA663−HA656 (mag)
NGC 6830-1	19:51:00.47	+23:06:50.6	0.10	−3.70	1.50	10.350	0.086	0.069	7.563	0.023
NGC 6830-2	19:50:58.55	+23:08:28.4	1.20	−3.00	1.50	10.412	0.151	0.064	7.679	0.047
NGC 6830-3	19:51:58.13	+22:44:59.8	−3.30	−7.00	3.70	11.806	0.159	0.316	9.458	−0.004
NGC 6830-4	19:50:02.31	+23:00:15.2	−3.60	−8.20	3.70	12.831	0.368	0.135	11.533	0.070
NGC 6830-5	19:50:05.02	+23:02:55.2	−2.50	−5.70	3.70	12.592	0.398	0.196	11.673	0.033
NGC 6830-6	19:50:04.61	+23:20:27.3	−7.60	0.10	3.70	13.473	0.405	0.132	11.715	0.053
NGC 6830-7	19:52:08.58	+22:59:59.8	4.10	−14.60	5.00	14.151	0.293	0.354	12.184	0.249
NGC 6830-8	19:50:02.94	+23:02:40.2	−3.00	−7.20	3.70	13.474	0.398	0.153	12.210	0.086
NGC 6830-9	19:52:10.97	+23:17:06.0	−0.80	−7.40	3.70	13.562	0.473	0.134	12.222	1.148
NGC 6830-10	19:52:25.39	+22:49:11.6	0.10	1.70	3.70	13.886	0.401	0.144	12.619	0.199
NGC 6830-11	19:51:07.65	+23:24:32.6	−3.10	−18.50	3.70	13.859	0.392	0.184	12.366	0.205

Note. Column 1: ID of candidates. Column 2: R.A. in the sexagesimal format (J2000). Column 3: decl. in the sexagesimal format (J2000). Column 4: proper motion of R.A. Column 5: proper motion of decl. Column 6: PM uncertainties. Column 7: K_s-band magnitudes adopted from 2MASS. Column 8: $J - H$. Column 9: $H - K_s$. Column 10: instrumental magnitude of the HA663 filter. Column 11: HA663−HA656 magnitude difference.

<div align="center">

Table 2
Observation Log and Results

</div>

ID	Date	Telescope	Instrument	Time	R-band	Type
NGC 6830-1	2014 May 1	Palomar 60 inch	SED Machine	300 s	11.19	Be
NGC 6830-2	2014 May 1	Palomar 60 inch	SED Machine	300 s	11.51	Be
NGC 6830-1	2014 Aug 2	Lulin 1 m	HIYOYU	1200 s	11.19	Be
NGC 6830-1	2015 Jun 15	Lick 3 m	Kast Dual Spectrograph	600 s	11.19	Be
NGC 6830-2	2015 Jun 15	Lick 3 m	Kast Dual Spectrograph	600 s	11.51	Be
NGC 6830-3	2015 Jun 15	Lick 3 m	Kast Dual Spectrograph	1200 s	13.24	Be
NGC 6830-4	2015 Jun 15	Lick 3 m	Kast Dual Spectrograph	1200 s	15.28	A
NGC 6830-5	2015 Jun 15	Lick 3 m	Kast Dual Spectrograph	1200 s	14.98	G
NGC 6830-6	2015 Jun 16	Lick 3 m	Kast Dual Spectrograph	1500 s	14.98	G
NGC 6830-7	2015 Jun 16	Lick 3 m	Kast Dual Spectrograph	1500 s	15.59	G
NGC 6830-8	2015 Jun 15	Lick 3 m	Kast Dual Spectrograph	1200 s	15.69	G
NGC 6830-9	2015 Jun 16	Lick 3 m	Kast Dual Spectrograph	1500 s	15.89	G
NGC 6830-10	2015 Jun 16	Lick 3 m	Kast Dual Spectrograph	1200 s	16.18	G
NGC 6830-11	2015 Jun 16	Lick 3 m	Kast Dual Spectrograph	1500 s	15.93	G

Note. Column 1: ID of targets. Column 2: Observations dates. Column 3: Telescope name. Column 4: Instrument name. Column 5: Exposure time in seconds. Column 6: R-band magnitudes adapted from PPMXL catalog. Column 7: Spectral types.

5. Selecting possible Be stars from emission-line candidates based on the $J - H$ versus $H - K_s$ color–color diagram (CMD). The gray contours as shown in Figure 1(d) represent the region of 1185 known Be stars (Zhang et al. 2005). Under the assumption that most Be stars have similar infrared colors, we identified Be star candidates as those in NGC 6830 inside the gray-dashed region in the CMD.

Using the above criteria, we identified 11 Be star candidates (Table 1). One candidate was confirmed as the known Be star VES 72 in the cluster NGC 6830 (listed as NGC 6830-2 in Table 1; Hoag & Applequist 1965).

3. SPECTROSCOPIC OBSERVATIONS AND DATA REDUCTION

3.1. SED-machine Observations

To demonstrate the feasibility and capability of the SED-machine in the study of Be stars, we obtained the optical spectra of two bright objects, VES 72 (NGC 6830-2) and a new Be star candidate NGC 6830-1 during its commission runs. Logs of observations are listed in Table 2. Due to time constraints during the commission runs, we only observed the 2 brightest candidates but not all of our 11 candidates. The SED-machine, mounted on the Palomar 1.5-m telescope, observations were carried out on 2014 May 1 under a seeing of approximately $2''$.

The SED-machine IFU spectra were reduced independently with the pipelines developed by the NCU and the Caltech PTF team. The IFU data reduction procedures consist of the following: (1) overscan and bias subtraction, (2) automatic spectrum identification using a Xe arc-lamp spectra image, (3) calculating wavelength calibration solutions of every IFU spectra using HgNeXe lamp sources, (4) simple-sum extraction of all spectra, (5) reconstructing the image of the sky as seen before the prism from surrounding sky identification, and (6) object spectrum extraction with sky spectra subtraction, wavelength calibration, and flux calibration.

3.2. Lulin 1-m Telescope (LOT) Observations

To confirm the Hα detection from SED-machine observations, we re-observed NGC 6830-1 using the Hiyoyu spectrograph on the LOT. The LOT observations were conducted on 2014 August 2 under a seeing of approximately $1''.5$. Using a grating of 300 mm^{-1} and a slit width of $2''$, we covered a wavelength range of 3800–7600 Å. The Hiyoyu spectrum was reduced with the IRAF[14] package, following the standard data reduction procedure, i.e., dark, bias-subtraced, flat-fielding-corrected, wavelength calibration, and flux calibration. The wavelength calibration was performed using a HeNeAr lamp. The flux calibration might not be very accurate due to the unstable weather during the observation.

3.3. Lick Observations

We used the Kast dual spectrograph on the 3-m Shane telescope at the Lick observatory to complete the confirmation of spectral typing of the 11 Be star candidates. The observing runs were conducted on 2015 June 15–16 under a seeing of $1''.5$–$2''$ using a $2''$ slit width. Using 600/7500 grating on the red side and 600/4310 grism on the blue side, we can cover a wavelength range of 3500–7800 Å. The dispersions on the red side and blue side are 2.32 and 1.85 Å pixel^{-1}, respectively. We reduced the spectra using the standard tools in IRAF, including corrections for overscan bias and flat-fielding using the dome flat images. We used NeHg-Cd arc lamps for wavelength calibrations and standard stars Feige 92 and BD +28 4211 for flux calibration.

4. RESULTS

4.1. SED-machine and LOT Spectra

In Figure 3, we showed the SED-machine spectra of the bright Be stars NGC 6830-1 and VES 72 (NGC 6830-2). The spectrum of VES 72 shows a prominent Hα emission line and clear hydrogen and He Iλ4471 + Mg IIλ4481 absorption lines. We further observed the new Be candidate NGC 6830-1 using

---

[14] Image Reduction and Analysis Facility. IRAF is written and supported by the National Optical Astronomy Observatories (NOAO) in Tucson, Arizona.
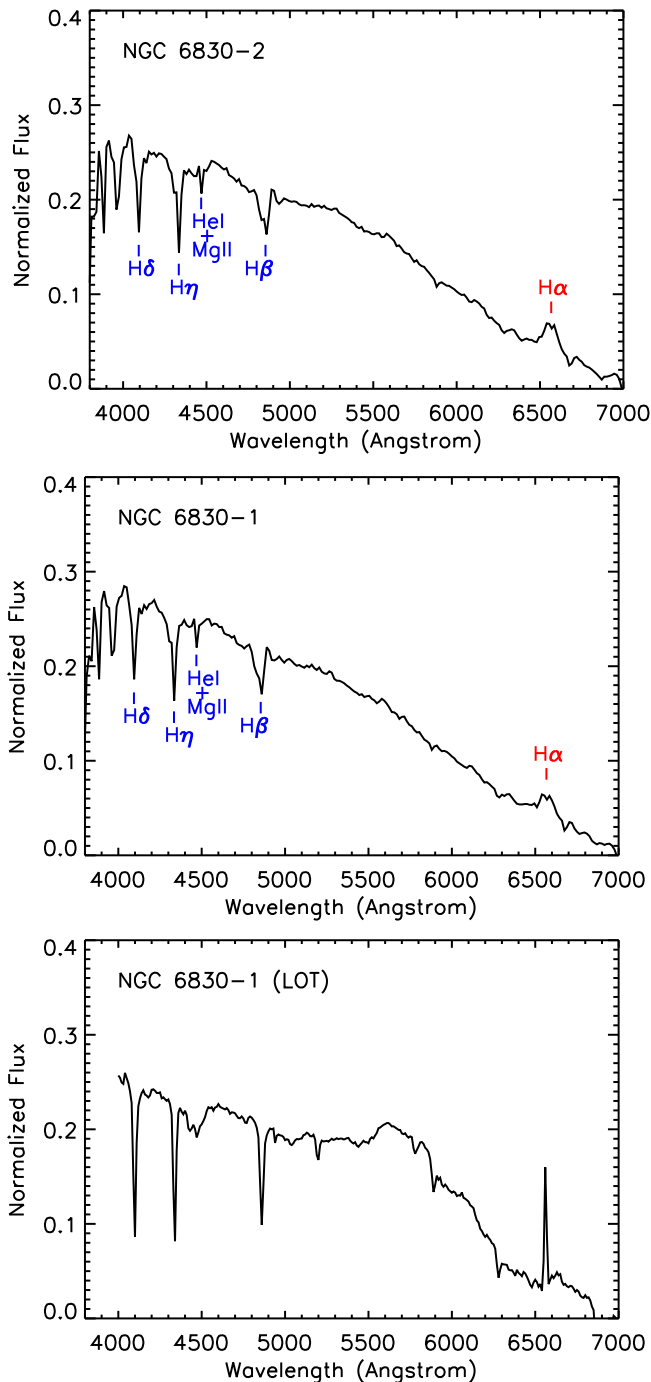
Figure 3. SED-machine results. The unit of the *y*-axis is normalized fluxes at 7000 Å in logarithm. Upper panel: SED-machine spectrum of the known Be star VES 72. We detect the clear Hα emission line while other Balmer series show absorption features. Middle panel: we also detected a clear Hα emission line for the Be star candidate NGC6830-1 with the SED-machine. Lower panel: the Hα emission line also appears in the LOT spectrum for the same candidate.

the SED-machine, and the Hiyoyu spectrograph mounted on the LOT. Both SED-machine and LOT spectra present a clear detection of the Hα emission line, and hydrogen and He I λ4471 + Mg II λ4481 absorption lines, indicating a Be-type. With a spectral resolution of $\lambda/\delta\lambda \sim 333$ of the Hiyoyu spectragraph, we estimated an equivalent width of the Hα emission-line, EW [Hα] = −5 Å for NGC 6830-1. Although the spectral

resolution is too poor to classify the spectral subtype, the similar brightness of NGC 6830-1 to VES 72 suggests similar subtypes (e.g., B6-type).

4.2. Lick Spectra

We present the spectra of Be star candidates obtained by the Lick 3 m Shane telescope in Figure 4. Only three Be star candidates (NGC6830-1, NGC6830-2, and NGC6830-3) show Hα emission and B-type spectra. All candidates are discussed in the following subsections.

4.2.1. Confirmed Be Stars

1. NGC 6830-1: this candidate shows a prominent Hα emission line with the EW[Hα] of −7 Å and hydrogen absorption lines of Hβ, Hγ, Hε, and Hδ. The EW[Hα] is similar to that of the LOT observation. It also shows He I λ4026, He I λ4387, and He I λ4471 + Mg II λ4481 absorption lines, the features of B-type stars. We thus confirmed the candidate as a newly discovered Be star.
2. NGC 6830-2: NGC6830 2 is a known Be star VES 72, a B6-type star with photoelectric observations (Hoag & Applequist 1965). We also detected the Hα emission line, with the EW[Hα] = −9 Å. It shows similar hydrogen and helium/magnesium absorptions lines as in NGC 6830-1.
3. NGC 6830-3: the star shows the Hα line in emission with the EW[Hα] = −8 Å. In addition to the same hydrogen and helium/magnesium absorption lines detected in NGC 6830-1 and NGC 6830-2, it also shows the He I λ4009 absorption line. We thus classified the star as a Be star. The star is 2 mag fainter than NGC 6830-1 and NGC 6830-2, implying a late-type B9 star.

4.2.2. Non-Be Star Candidates

1. NGC 6830-4: we do not detect the Hα emission line for the star, and it shows the Ca II K absorption line, indicating the star might be a late-A or F-type star.
2. NGC 6830-5: it shows not only the Ca II K absorption line, but also the G-band absorption at 4300 Å. The star is classified as a G-type star.
3. NGC 6830-6–NGC 6830-11: compared to NGC 6830-5, these stars show stronger G-band absorption, and weaker Hγ and Hε absorption lines. We classify NGC 6830-6–NGC 6830-11 as G-type stars.

4.3. Infrared Color

The Be star NGC 6830-3 shows an infrared excess $H - K_s = 0.316$ (Figure 1(d)), as in many known Be stars. Such infrared excess can be explained by free–free emission from circumstellar disks (Lee & Chen 2011). For comparison, we included the fluxes of 3.4 μm (W1), 4.6 μm (W2), 12 μm (W3), and 22 μm (W4) from the *Wide-field Infrared Survey Explorer* (*WISE*; Wright et al. 2010), and plotted in Figure 5 the spectral energy distribution between 0.4 and 25 μm of three Be stars (Table 3). All of the objects have no significant 22 μm detection, suggesting no presence of warm dust. Although the detection is only an upper limit, it seems that NGC 6830-3 might have a different W3−W4 color from NGC 6830-1 and NGC 6830-2. Observations with high resolution and sensitivity are in demand to confirm the 22 μm detection in NGC 6830-3 in the future.
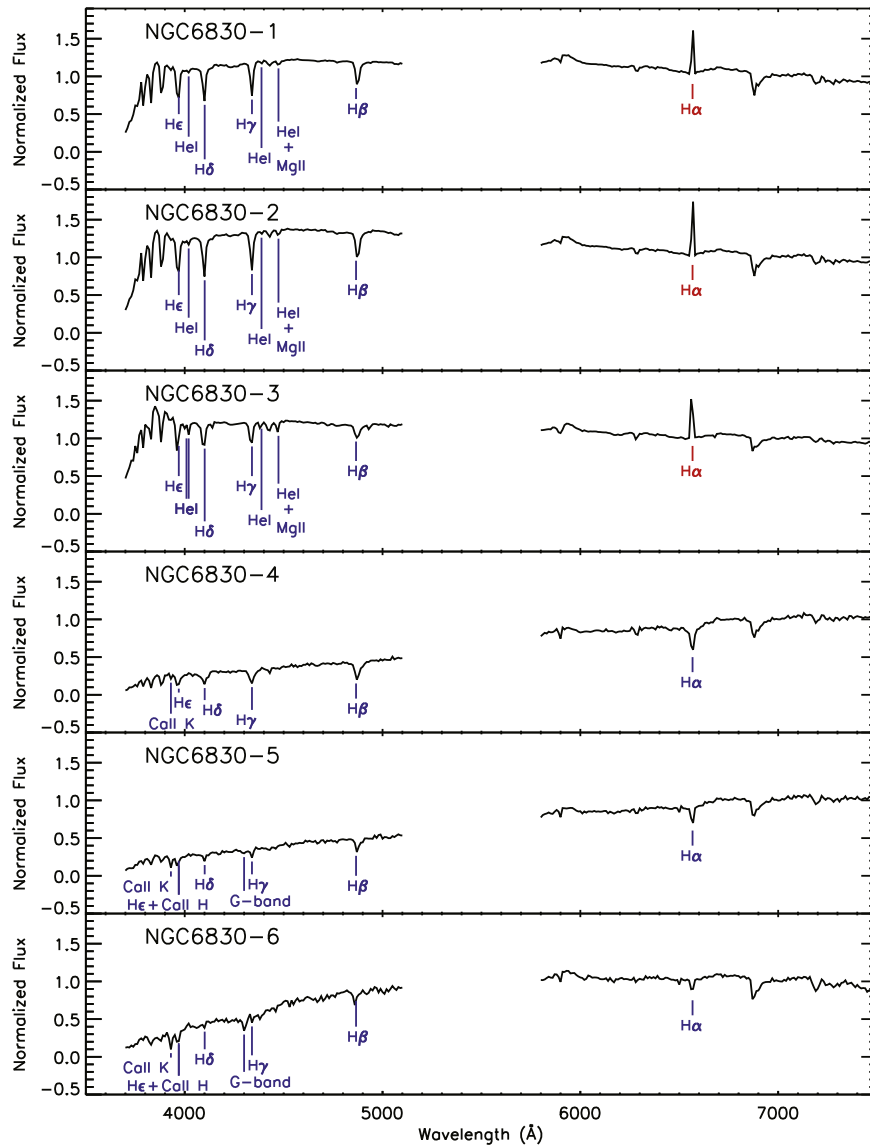
Figure 4. Lick spectra of Be star candidates. Fluxes are normalized at 7000 Å.

4.4. Optical Variability

Be stars are also known as photometric and spectroscopic variables. Their variabilities show a wide range of timescales from much less than a day (Percy et al. 2002) to more than several decades (Okazaki 1997). Compare to normal B-type stars, photometric irregular variation is frequently seen in Be stars (Kourniotis et al. 2014). There are three types of variability found in Be stars: (1) short-term variability with timescales of days (Hubert et al. 1997); (2) mid-term variability with timescales of days and weeks with the amplitude of 0.3 mag (Okazaki 1997; Hubert & Floquet 1998); (3) long-term variability with timescales of years and larger amplitudes of >0.3 mag (Hubert & Floquet 1998). Since the PTF R-band light curve data saturated around the 14th magnitude, we adopted the V-band light curve data from the All Sky Automated Survey (ASAS; Pojmański 2002) to investigate the variability of our detected Be stars. The ASAS is a project to monitor stars brighter than 14 mag to investigate their photometric variability; thus it is suitable to search for long-term variability with large amplitude >0.3 mag for Be stars.

We chose two stars, star1 and star2 in the same field, as the photometric references to build up the light curves using the differential photometry technique. We only used the data with grade A from the ASAS catalog, i.e., the best data with photometric uncertainties <0.05 mag in the catalog. The value $\sigma_{\rm sc}$ was defined as the standard deviation of magnitude difference between the reference and the Be stars, and used to determine the significance of the variability. The $\sigma_{\rm sc}$ against star1 and star2 of NGC6830-1, NGC6830-2, and NGC6830-3 are 0.15 and 0.14, 0.14, and 0.16, and 0.26 and 0.23 mag, respectively (Figure 6). These $\sigma_{\rm sc}$ values are all comparable to the systematic errors of corresponding magnitudes in ASAS (Pojmański 2002). Therefore, we do not detect any significant long-term variability in the optical band for these three Be stars.

5. SUMMARY AND DISCUSSION

In summary, we apply PTF's Hα imaging photometry to identify 11 Be star candidates in NGC 6830. Three stars have been confirmed as Be stars with intermediate and late-type spectra by using the SED-machine on the Palomar 1.5 m
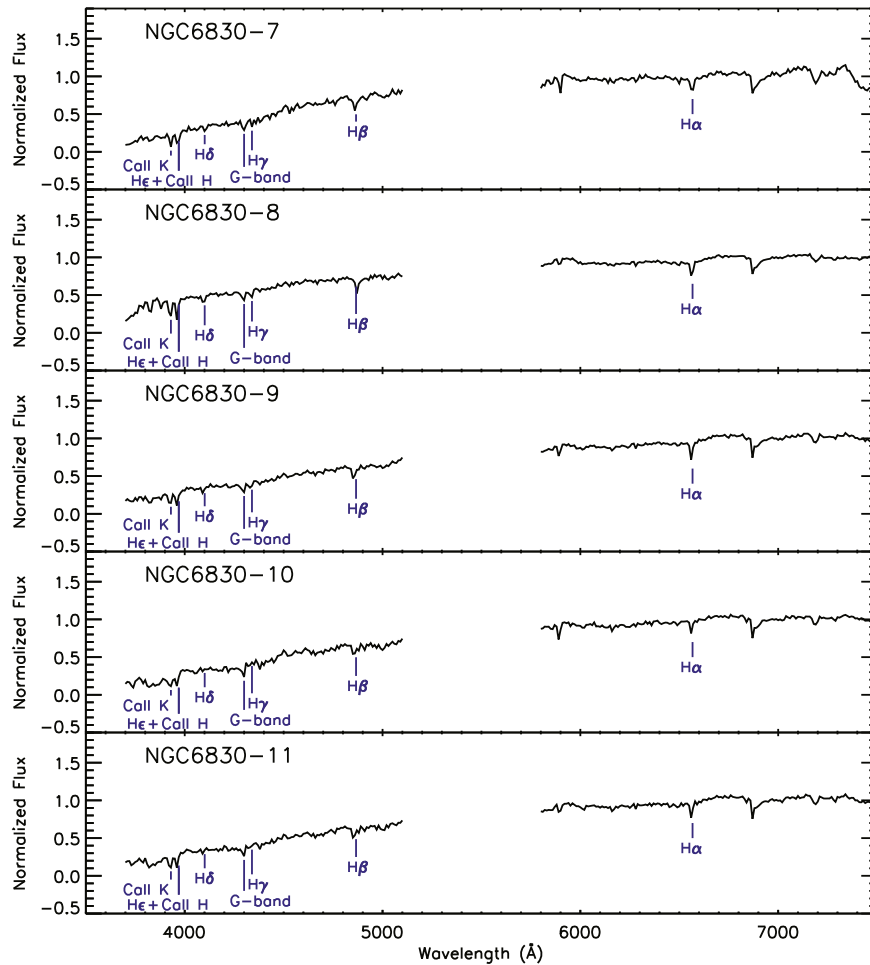
Figure 4. (Continued.)

telescope, the Hiyoyu spectrograph on the Lulin 1-m telescope, and the Kast dual spectrograph on the Lick 3-m telescope. We suggest that there are three Be stars in the cluster NGC 6830. The spatial distribution of the Be stars might be caused by gravitational disruption over time. We also present the results of the SED-machine; this study demonstrated that the high efficiency of the SED-machine can provide rapid observations for Be stars in a comprehensive survey in the future.

We suggest that there are three Be stars in the cluster NGC 6830. McSwain & Gies (2005) studied the fraction of Be stars in eight clusters with an age older than 100 Myr; only four clusters have up to two Be stars. These results indicate that old open clusters lack Be stars. Although our results are consistent with the previous conclusions, it should be noted that either the relaxation process or Galactic external perturbation (Chen et al. 2004) might have happened in open clusters. As shown in Figure 7, the Be star NGC6830-3 is located in the outer region of the cluster, while NGC6830-1 and NGC6830-2 are located in the central region. With an age of 125 Mys, the open cluster NGC 6830 might have a very irregular shape and become loose. The spatial distribution of Be stars could be the consequence of the relaxation process. Since McSwain & Gies (2005) searched Be stars within a fixed angular size, more Be stars could be discovered if a larger size is used.

Dachs et al. (1988) proposed an empirical relation between the disk fraction f_D and the EW[Hα] for Be stars:

$$f_D \simeq 0.1 \times \frac{\mathrm{EW}[\mathrm{H}\alpha]}{-30\,\text{Å}}, \tag{1}$$

where f_D is the ratio of disk radiation to total radiation of the star-disk system. The EW[Hα] of the Be stars in NGC 6830 are all greater than $-10\,\text{Å}$, suggesting the disk fraction $f_D < 0.03$. The result is consistent with Dachs et al. (1988), who showed that most late-type Be stars (B4–B7) have $f_D < 0.1$, while most early-type Be stars (B1–B3) have $f_D > 0.1$.

Several mechanisms might cause long-term variability in Be stars: (1) long-lived strong outbursts (Hubert & Floquet 1998), (2) the decline of brightness due to the cooling envelope (Koubský et al. 1997), and (3) a weak brightness change related to Hα variability. The brightness of NGC 6830-1 and NGC 6830-2 allow us to investigate the variability with the amplitude larger than 0.15 mag using the ASAS data set. We do not discover any significant variability for NGC 6830-1 and NGC 6830-2. This is consistent with the previous studies; Hubert & Floquet (1998) showed that only 12% of B6-type Be stars have the variability with the amplitude of 0.12–0.3 mag. Because large amplitude caused by strong outbursts is usually
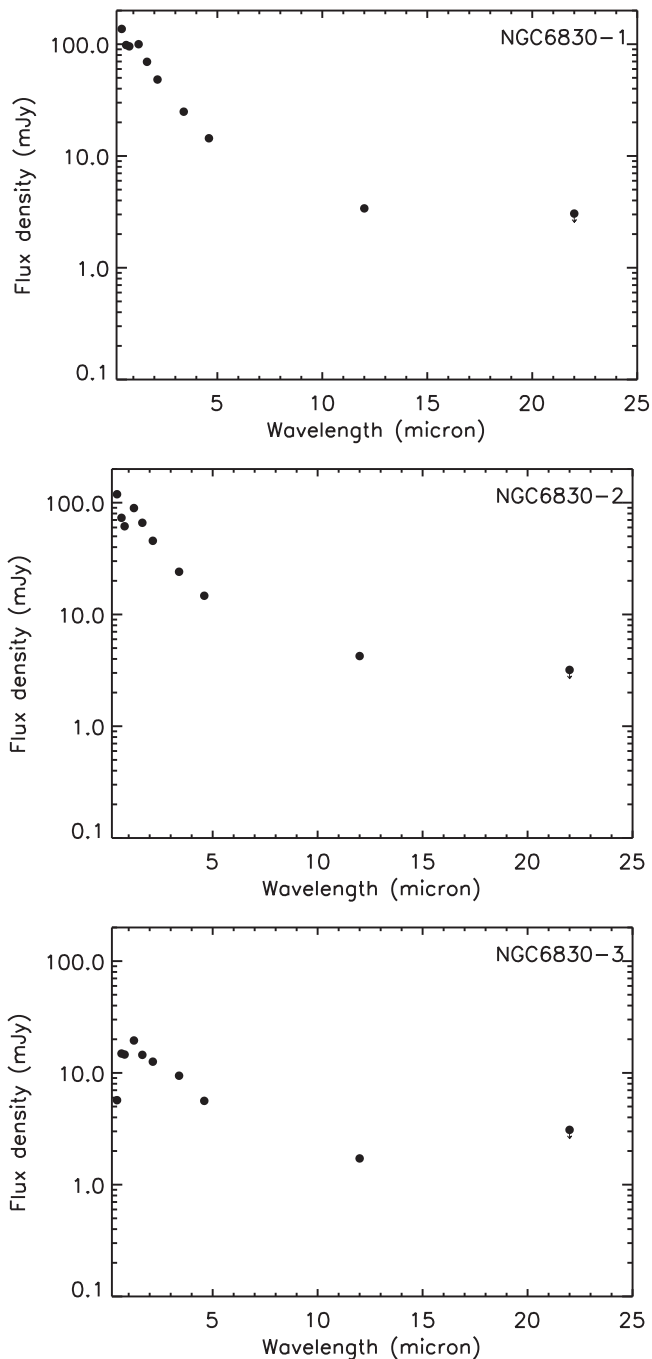
Figure 5. Spectral energy distribution between 0.4 and 25 μm. Detections at 22 μm for these Be stars are upper limits. Flux densities of 445, 658, and 806 nm are adopted from PPMXL; flux densities of 1.25, 1.65, and 2.15 μm are adopted from 2MASS; 3.4, 4.6, 12, and 22 μm flux densities are adopted from *WISE*.
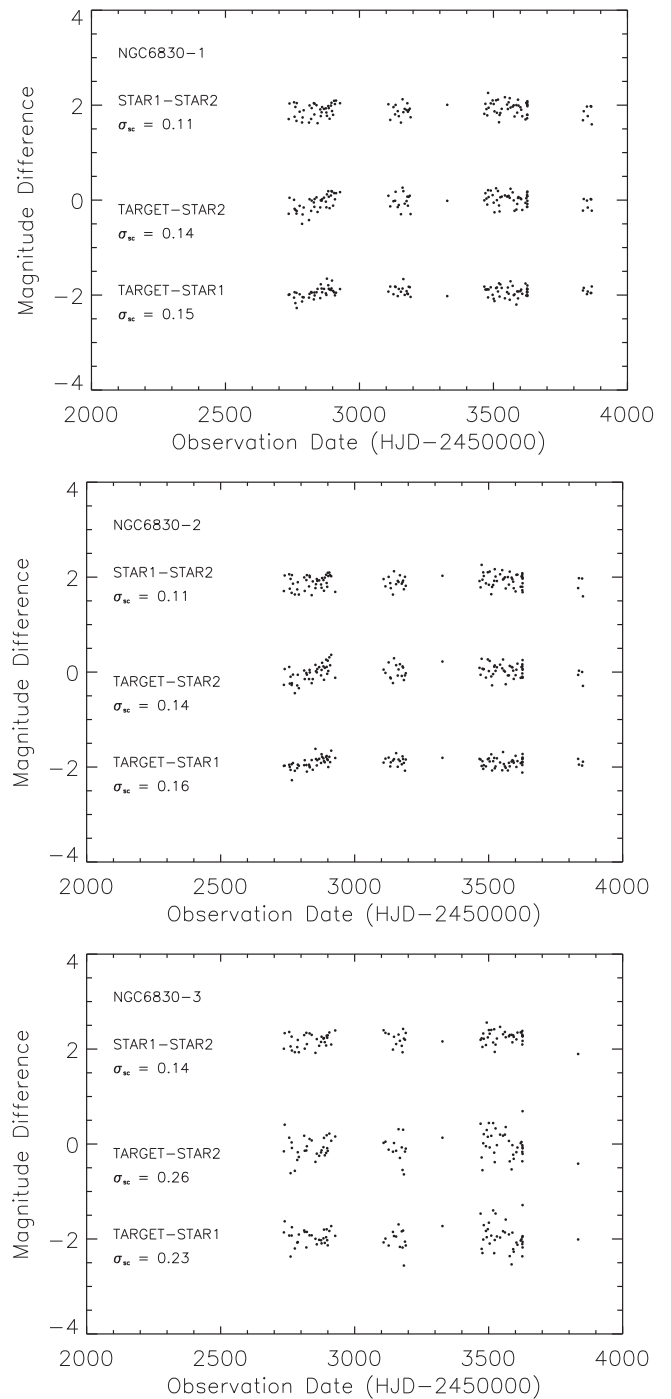

Figure 6. Differential photometry of Be stars in NGC 6830.

Table 3
Flux Density of Be Stars in NGC 6830

ID	0.445 μm (mJy)	0.658 μm (mJy)	0.806 μm (mJy)	1.25 μm (mJy)	1.65 μm (mJy)	2.2 μm (mJy)	3.4 μm (mJy)	4.6 μm (mJy)	12 μm (mJy)	22 μm (mJy)
NGC 6830-1	137	98.3	95.7	100	69.6	48.3	24.9	14.4	3.397	3.053
NGC 6830-2	119	73.2	61.5	89.5	66.1	45.6	24.1	14.7	4.245	1.717
NGC 6830-3	5.7	14.9	14.6	19.5	14.5	12.6	9.434	5.621	1.717	3.093

Note. Column 1: ID of targets. Column 2 to 11: Flux density in millijansky adopted from the PPMXL, 2MASS, and *WISE* catalogs. The detections at 22 μm for three Be stars are upper limits.
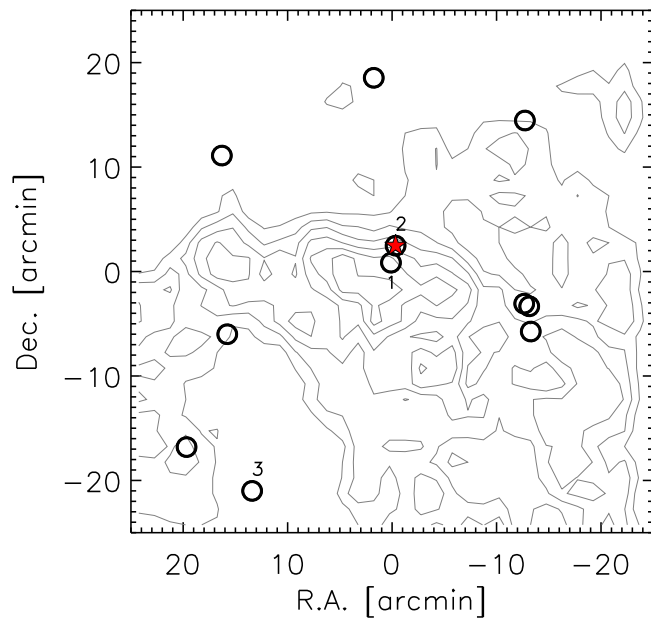
Figure 7. Spatial distribution of Be star candidates. The open circles: Be star candidates; red pentagram: the known Be star VES 72. Contours represent the distribution of stars within a field of $50' \times 50'$.
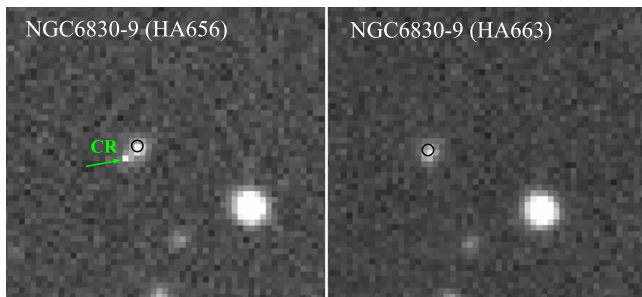
Figure 8. HA656 (left) and HA663 (right) images of NGC6830-9. The green arrow indicates the residual cosmic-ray. Black open circles represent the position of NGC 6830-9.

seen in the earliest Be stars, it is not surprising that we do not detect variability in these Be stars.

Finally, as a pilot project to search for Be stars in clusters with different ages, we reviewed our selection criteria for NGC 663 (Yu et al. 2015) and in this work. Of the 11 Be candidates, 8 are classified as A- or G-type stars; most of them have marginal Hα detection in the HA663−HA656 color diagram (Figure 2). This misidentification can be improved by using the 2MASS color–color diagram. As shown in Figure 1(d), if we cause the selection region (dashed line) to have a similar range as the known Be stars, most G-type stars would have been ruled out. Thus, we will change our selection criteria in our future project. Moreover, it should be noted that the star NGC6830-9 has a large Hα excess in Figure 2, while the optical spectrum suggested a G-type star with the Hα absorption line. This is caused by the contamination of a residual cosmic-ray hitting on the target region, which is not easy to eliminate. Procedures for removing cosmic-rays around science targets will be performed carefully in a future project.

REFERENCES

Barkhatova, K. A. 1957, SvA, 1, 822
Ben-Ami, S., Konidaris, N., Quimby, R., et al. 2012, Proc. SPIE, 8446, 86
Carciofi, A. C., & Bjorkman, J. E. 2006, ApJ, 639, 1081
Carciofi, A. C., Okazaki, A. T., le Bouquin, J.-B., et al. 2009, A&A, 504, 915
Chen, W. P., Chen, C. W., & Shu, C. G. 2004, AJ, 128, 2306
Chojnowski, S. D., Whelan, D. G., Wisniewski, J. P., et al. 2015, AJ, 149, 7
Cutri, R. M., Skrutskie, M. F., van Dyk, S., et al. 2003, yCat, 2246, 0
Dachs, J., Kiehling, R., & Engels, D. 1988, A&A, 194, 167
de Mink, S. E., Langer, N., Izzard, R. G., Sana, H., & de Koter, A. 2013, ApJ, 764, 166
Drew, J. E., Greimel, R., Irwin, M. J., et al. 2005, MNRAS, 362, 753
Fabregat, J., & Torrejón, J. M. 2000, A&A, 357, 451
Girardi, L., Bertelli, G., Bressan, A., et al. 2002, A&A, 391, 195
Hoag, A. A., & Applequist, N. L. 1965, ApJS, 12, 215
Hubert, A. M., & Floquet, M. 1998, A&A, 335, 565
Hubert, A. M., Floquet, M., Hao, J. X., et al. 1997, A&A, 324, 929
Jaschek, C., Jaschek, M., & Kucewicz, B. 1964, ZA, 59, 108
Keller, S. C., Grebel, E. K., Miller, G. J., & Yoss, K. M. 2001, AJ, 122, 248
Kharchenko, N. V., Piskunov, A. E., Schilbach, E., Röser, S., & Scholz, R.-D. 2012, A&A, 543, 156
Kharchenko, N. V., Piskunov, A. E., Schilbach, E., Röser, S., & Scholz, R.-D. 2013, A&A, 558, A53
Koubský, P., Harmance, P., Kubát, J., et al. 1997, A&A, 328, 551
Kourniotis, M., Bonanos, A. Z., Soszyński, I., et al. 2014, A&A, 562, 125
Kraus, S., Monnier, J. D., Che, X., et al. 2012, ApJ, 744, 19
Laher, R. R., Surace, J., Grillmair, C. J., et al. 2014, PASP, 126, 674
Law, N. M., Kulkarni, S. R., Dekany, R. G., et al. 2009, PASP, 121, L1395
Lee, C.-D., & Chen, W.-P. 2011, in IAU Symp. 272, Active OB stars: structure, evolution, mass loss, and critical limit, ed. C. Neiner, G. Wade, G. Meynet, & G. Peters (Cambridge: Cambridge Univ. Press), 366
Lee, U., Osaki, Y., & Saio, H. 1991, MNRAS, 250, 432
Lin, C. C., Hou, J. L., Chen, L., et al. 2015, RAA, 15, 8
Martayan, C., Baade, D., & Fabregat, J. 2010, A&A, 509, 11
Mathew, B., & Subramaniam, A. 2011, BASI, 39, 517
Mathew, B., Subramaniam, A., & Bhatt, B. C. 2008, MNRAS, 388, 1879
Mclaughlin, D. B. 1932, POMic, 4, 175
McSwain, M. V., & Gies, D. R. 2005, ApJS, 161, 118
McSwain, M. V., Huang, W., & Gies, D. R. 2009, ApJ, 700, 1216
Meilland, A., Millour, F., Kanaan, S., et al. 2012, A&A, 538, 110
Ngeow, C. C., Konidaris, N., Quimby, R., et al. 2013, in IAU Symp. 290, Feeding Compact Objects: Accretion on All Scales, ed. C. M. Zhang, T. Belloni, M. Méndez, & S. N. Zhang (Cambridge: Cambridge Univ. Press), 281
Okazaki, A. T. 1997, A&A, 318, 548
Peña, J. H., Machado, L. F., Garcia, H., et al. 2011, RMxAA, 47, 309
Percy, J. R., Hosick, J., Kincaide, H., & Pang, C. 2002, PASP, 114, 551
Pojmañski, G. 2002, AcA, 52, 397
Pols, O. R., Cotē, J., Waters, L. B. F. M., & Heise, J. 1991, A&A, 241, 419
Porter, J. M., & Rivinius, T. 2003, PASP, 115, 1153
Quirrenbach, A., Bjorkman, K. S., Bjorkman, J. E., et al. 1997, ApJ, 479, 477

Quirrenbach, A., Buscher, D. F., Mozurkewich, D., Hummel, C. A., &
Armstrong, J. T. 1994, A&A, 283, L13
Raddi, R., Drew, J. E., Steeghs, D., et al. 2015, MNRAS, 446, 274
Ritter, A., Ngeow, C. C., Konidaris, N., Quimby, R., & Ben-Ami, S. 2014,
CoSka, 43, 209
Rivinius, T., Baade, D., & Štefl, S. 2003, A&A, 411, 229
Rivinius, T., Carciofi, A. C., & Martayan, C. 2013, A&ARv, 21, 69
Röser, S., Demleitner, M., & Schilbach, E. 2010, AJ, 139, 2440

Shao, Y., & Li, X. D. 2014, ApJ, 796, 37
Townsend, R. H. D., Owocki, S. P., & Howarth, I. D. 2004, MNRAS, 350, 189
Wisniewski, J. P., & Bjorkman, K. S. 2006, ApJ, 652, 458
Wood, K., Bjorkman, K. S., & Bjorkman, J. E. 1997, ApJ, 477, 926
Wright, E. L., Eisenhardt, P. R. M., Mainzer, A. K., et al. 2010, AJ,
140, 1868
Yu, P.-C., Lin, C. C., Chen, W. P., et al. 2015, AJ, 149, 43
Zhang, P., Chen, P. S., & Yang, H. T. 2005, NewA, 10, 325